

# Genetic basis and molecular mechanism for idiopathic ventricular fibrillation

Qiuyun Chen<sup>\*†</sup>, Glenn E. Kirsch<sup>†‡</sup>, Danmei Zhang<sup>\*†</sup>, Ramon Brugada<sup>§</sup>, Josep Brugada<sup>||</sup>, Pedro Brugada<sup>¶</sup>, Domenico Potenza<sup>#</sup>, Angel Moya<sup>\*\*</sup>, Martin Borggrefe<sup>\*\*</sup>, Günter Breithardt<sup>\*\*</sup>, Rocio Ortiz-Lopez<sup>\*</sup>, Zhiqing Wang<sup>††</sup>, Charles Antzelevitch<sup>‡‡</sup>, Richard E. O'Brien<sup>\*</sup>, Eric Schulze-Bahr<sup>\*\*</sup>, Mark T. Keating<sup>§§</sup>, Jeffrey A. Towbin<sup>\*†|||</sup> & Qing Wang<sup>\*</sup>

<sup>\*</sup> Department of Pediatrics (Cardiology), <sup>§</sup> Medicine (Cardiology),

<sup>††</sup> Cardiovascular Sciences, <sup>|||</sup> Molecular and Human Genetics, Baylor College of Medicine, Houston, Texas 77030, USA

<sup>‡</sup> The Rammelkamp Center for Research, MetroHealth Campus, Case Western Reserve University, Cleveland, Ohio 44109, USA

<sup>||</sup> Arrhythmia Unit, Cardiovascular Institute, Hospital Clinic, University of Barcelona, 08036 Barcelona, Spain

<sup>¶</sup> the Cardiovascular Center, OLV Hospital, 9300 Aalst, Belgium

<sup>#</sup> Cardiology Department, IRCCS Casa Sollievo della Sofferenza, S. Giovanni Rotondo, Italy

<sup>\*</sup> Department of Cardiology, Hospital Vall d'Hebron, 08020 Barcelona, Spain

<sup>\*\*</sup> Department of Cardiology and Angiology, Institute of Arteriosclerosis Research, Hospital of the University of Munster, D48129 Munster, Germany

<sup>‡‡</sup> Masonic Medical Research Laboratory, Utica, New York 13504, USA

<sup>§§</sup> Howard Hughes Medical Institute, Department of Human Genetics and Medicine, University of Utah, Salt Lake City, Utah 84112, USA

<sup>†</sup> These authors contributed equally to this work.

Ventricular fibrillation causes more than 300,000 sudden deaths each year in the USA alone<sup>1,2</sup>. In approximately 5–12% of these cases, there are no demonstrable cardiac or non-cardiac causes to account for the episode, which is therefore classified as idiopathic ventricular fibrillation (IVF)<sup>3–6</sup>. A distinct group of IVF patients has been found to present with a characteristic electrocardiographic pattern<sup>7–15</sup>. Because of the small size of most pedigrees and the high incidence of sudden death, however, molecular genetic studies of IVF have not yet been done. Because IVF causes cardiac rhythm disturbance, we investigated whether malfunction of ion channels could cause the disorder by studying mutations in the cardiac sodium channel gene *SCN5A*. We have now identified a missense mutation, a splice-donor mutation, and a frameshift mutation in the coding region of *SCN5A* in three IVF families. We show that sodium channels with the missense mutation recover from inactivation more rapidly than normal and that the frameshift mutation causes the sodium channel to be non-functional. Our results indicate that mutations in cardiac ion-channel genes contribute to the risk of developing IVF.

Ventricular fibrillation is the most common cause of sudden cardiac death. When it occurs, there is no cardiac output, peripheral pulses and blood pressure are absent, and the patient loses consciousness. Death is imminent unless the arrhythmia is immediately controlled. IVF patients account for 3% of survivors of out-of-hospital cardiac arrest<sup>16</sup>. For patients who survive an episode of IVF, the rate of recurrence can be as high as 25–30% (refs 7, 17). A distinct electrocardiograph (ECG) feature, with right bundle branch block (RBBB) and elevation in ST segment in leads V1 to V3, has been described for some patients with sudden and aborted cardiac death due to IVF<sup>7–15</sup>. Although the exact prevalence of IVF associated with RBBB and ST segment elevation is not known, clinical experience in Belgium and Spain suggests that it accounts for 40–60% of all IVF cases (data not shown).

We studied six small families and two sporadic patients with IVF by using single-strand conformation polymorphism (SSCP) and

DNA sequence analyses to identify mutations in known ion channel genes, including the cardiac sodium channel gene *SCN5A*. Two aberrant SSCP conformers were identified in all affected members in family K005, one in exon 21 of *SCN5A* (data not shown) and the other in exon 28 (Fig. 1a, b)<sup>18</sup>. Neither of the SSCP anomalies was seen in unaffected individuals (Fig. 1b) or in DNA samples from more than 150 control individuals (data not shown). DNA sequence analysis revealed two C-to-T base substitutions, one in exon 21 and the other in exon 28 (Fig. 1c): these mutations lead to substitution of an arginine by a tryptophan at codon 1,232 (represented as R1232W; data not shown), which lies in the extracellular loop between transmembrane segments S1 and S2 of domain III, and to substitution of a highly conserved threonine by a methionine at codon 1,620 (T1620M; Fig. 1c) in the extracellular loop between S3 and S4 of domain IV. Studies with sodium-channel-specific toxins indicated that the extracellular loop between DIVS3 and DIVS4 is important for coupling channel activation to fast inactivation<sup>19–21</sup>.

Additional *SCN5A* mutations were found in two IVF families, K007 and K2823. Aberrant SSCP conformers were identified in affected individuals of K007 (Fig. 2a) and K2823 (Fig. 2b), but not in DNA samples from more than 150 control individuals (data not shown). DNA sequencing revealed that the abnormal SSCP band identified in K007 contained an insertion of two nucleotides, AA, which disrupted the splice-donor sequence of intron 7 (refs 18, 22) (Fig. 2a). The abnormal band identified in K2823 contained a deletion of a single nucleotide (A) at codon 1,397 (Fig. 2b). This deletion results in an in-frame stop codon that eliminates DIII/S6, DIV/S1–S6, and the carboxy-terminal portion of the cardiac sodium channel (Fig. 2b).

The potential contribution of R1232W and T1620M mutations to the mechanism of IVF was determined by heterologous expression

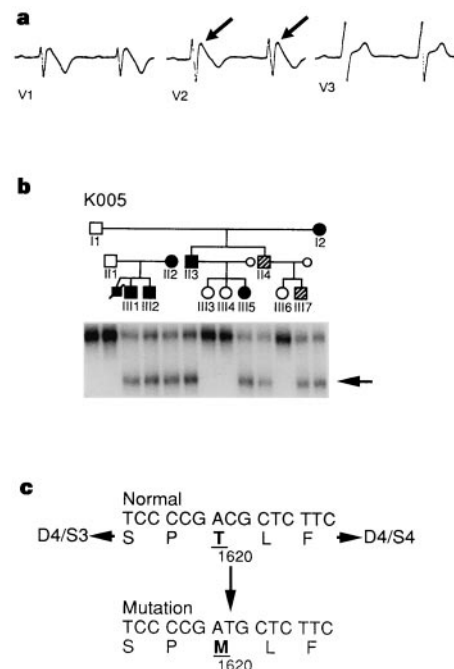


**Figure 1** *SCN5A* missense mutation co-segregating with IVF in family K005. **a**, Electrocardiogram of an affected individual (III1). Note the ECG pattern of RBBB and ST segment elevation (diagonal arrows) in leads V1–V3. **b**, Pedigree structure and SSCP analysis with primers amplifying exon 28 of *SCN5A*. Affected individuals are filled circles (females) and filled squares (males). Unaffected individuals are empty symbols, and individuals without clinical data are shown as hatched. The individual who suffered sudden death from IVF is slashed. **c**, DNA and amino-acid sequences of the *SCN5A* missense mutation associated with IVF in K005. DNA sequence analysis revealed a C-to-T substitution which causes the T1620M mutation in the extracellular loop between DIVS3 and DIVS4.

in *Xenopus* oocytes. Current–voltage families were recorded from wild-type (WT) and mutated (R/W + T/M, containing both amino-acid substitutions R1232W and T1620M) channels. Peak conductance–voltage plots that represent steady-state activation (Fig. 3a) were indistinguishable between the two types of channel. The voltage dependence of steady-state inactivation (Fig. 3a), however, was shifted nearly 10 mV towards more positive potentials in R/W + T/M channels compared with WT channels, with no change in the slope of the curve. When fitted to a Boltzmann distribution, the midpoint potentials were  $-72.6$  and  $-63.4$  mV respectively in WT and R/W + T/M channels. We observed no other differences in steady-state gating properties of the two channels. In particular, unlike *SCN5A* mutations associated with long-QT syndrome<sup>23–26</sup> (Fig. 4), no persistent, inactivation-resistant currents were observed in R/W + T/M channels (data not shown). These data confirm that IVF with RBBB and ST-segment elevation is a defect distinct from long-QT syndrome, which is a cardiac repolarization disorder characterized by a prolonged Q–T interval on ECG and a specific ventricular tachycardia, *torsade de pointes*.

Shifts in the voltage dependence of inactivation, unaccompanied by corresponding shifts in activation, suggested a change in the kinetics of inactivation. Therefore, we measured the time course of recovery from inactivation at negative potentials (Fig. 3b). At a recovery potential ( $V_r$ ) of  $-80$  mV, R/W + T/M channels showed a significantly faster recovery than wild-type channels. The time constant of the recovery process was markedly accelerated by more negative recovery potentials, and the difference between mutant and normal channels disappeared at potentials more negative than  $-110$  mV. In channels that were mutated at either R1232 or T1620, the R1232W mutant behaved most like normal channels whereas the T1620M mutant closely followed the kinetic pattern of the double (R/W + T/M) mutant (Fig. 3b). This indicates that T1620M is the mutation that is probably responsible for the IVF phenotype and that R1232W could be a rare polymorphism. In summary, biophysical analysis of the two missense mutations in *SCN5A* showed a shift in the voltage dependence of steady-state inactivation towards more positive potentials associated with a 25–30% acceleration in recovery time from inactivation at potentials near  $-80$  mV.

Genetic analysis demonstrated that all affected individuals in K005 carried two substitutions (T1620M and R1232W) on one chromosome and none on the other chromosome, suggesting that IVF in this family is inherited as an autosomal dominant trait. The presence of both normal and mutated sodium channels in the same tissue would promote heterogeneity of the refractory period, a well established mechanism in arrhythmogenesis, and therefore may be the underlying molecular defect that causes re-entrant arrhythmia in the IVF family K005.

The functional consequences of the splicing mutation have not been established. In view of the location of the mutation, within the intracellular loop between DIS2 and DIS3 (Fig. 4), it may reduce the number of functional sodium channels in IVF patients. The one-base-pair (1-bp) deletion in K2823 results in an intragenic stop codon which generates a truncated sodium channel with transmembrane domains DI, DII and part of DIII (Fig. 4). When tested in *Xenopus* oocytes, mutant RNA failed to express sodium currents (data not shown). Similar findings have been reported in rat brain sodium channels<sup>27</sup>. These results indicate that all four transmembrane domains are required for formation of a functional sodium channel.

Inhibition of the sodium channel current causes heterogeneous loss of the action potential dome in the right ventricular epicardium, leading to a marked dispersion of repolarization and refractoriness, an ideal substrate for the development of re-entrant arrhythmia<sup>28,29</sup>. Phase 2 re-entry produced by the same substrate is thought to provide the premature beat that initiates ventricular tachycardia and fibrillation. Both the splicing mutation and the

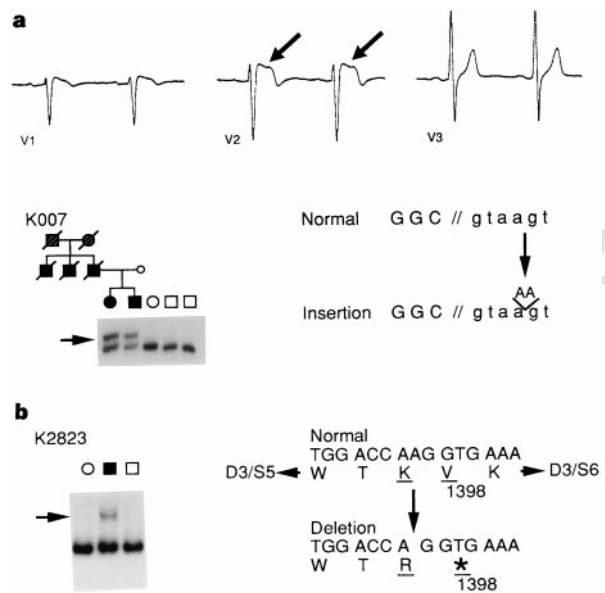


**Figure 2** *SCN5A* splicing mutation in K007 and intragenic deletion in K2823. **a**, *SCN5A* splicing mutation in K007 and electrocardiogram obtained from the male affected individual (proband) in K007. Pedigree structure and the abnormal SSCP conformers (indicated by an arrow) are shown. DNA sequence analysis of the normal and abnormal conformers in K007 revealed a two-base-pair (AA) insertion. This insertion occurs in the splicing donor site of intron 7 of *SCN5A*. The symbol // indicates the exon–intron boundary. **b**, A deletion of a single nucleotide A was identified in the abnormal SSCP band of K2823. The deletion causes a frameshift and leads to the premature termination of the cardiac sodium channel starting in the pore region of transmembrane domain III. The electrocardiogram for the proband in K2823 is not shown because the patient presented mild J point depression anteriorly with a rapidly upslping ST segment during a peak exercise, but not at the baseline.

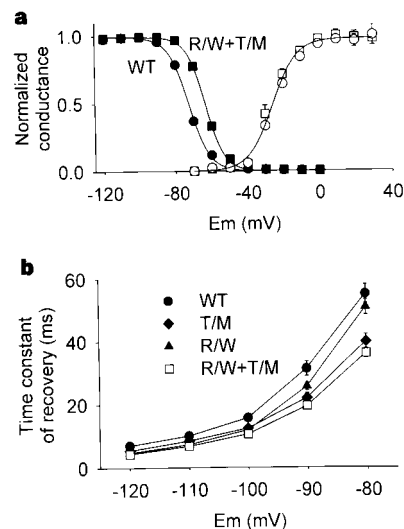


**Figure 3** Voltage-dependence of activation and inactivation, and time course of recovery from inactivation. **a**, Steady-state voltage-dependence of activation and inactivation in normal and mutated sodium channels. Open symbols: activation in wild-type (WT, open circles;  $n = 7$ ) and mutant (R/W + T/M, open squares;  $n = 7$ ) channels fit to a Boltzmann distribution with midpoint  $-25.4$  mV and slope factor  $6.5$  mV. Filled symbols: inactivation in WT (filled circles;  $n = 7$ ) and mutant channels (filled squares;  $n = 7$ ; error bars smaller than symbols) fit to Boltzmann distributions with midpoint potentials of  $-72.6$  and  $-63.4$  mV (slope factors of  $5.5$  and  $5.2$  mV), respectively in WT and R/W + T/M channels. **b**, Time course of recovery from inactivation. Average time constants versus recovery potential ( $V_r$ ) for WT (filled circles;  $n = 9$ ) and mutant channels: T/M (filled diamonds;  $n = 6$ ), R/W (filled triangles;  $n = 8$ ) and R/W + T/M (open squares;  $n = 5$ ).

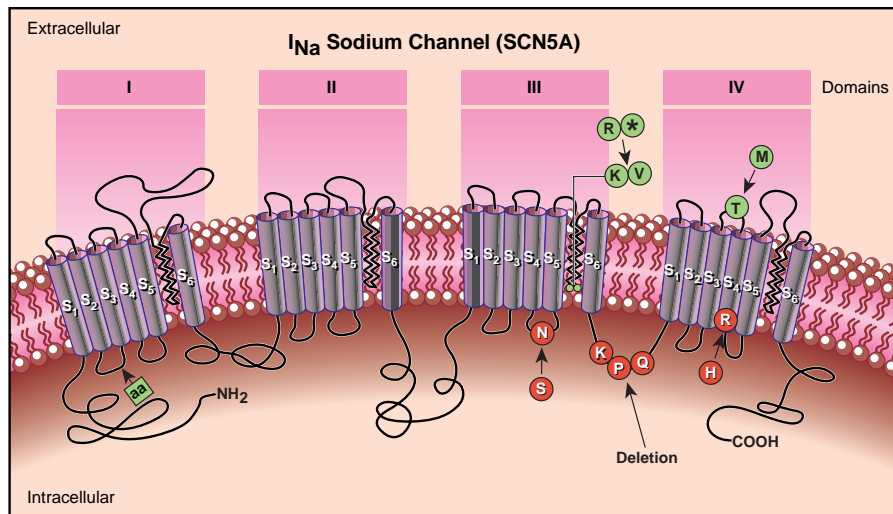


**Figure 4** The predicted secondary structure of the cardiac sodium channel and locations of mutations causing IVF and chromosome-3-linked long-QT syndrome (LQT). The channel consists of four putative transmembrane domains (DI–DIV),

one-nucleotide deletion result in a reduction in the number of functional sodium channels, which should promote the development of re-entrant arrhythmias.

This work shows that IVF with RBBB and ST segment elevation is a distinct syndrome and that mutations in the cardiac sodium channel gene *SCN5A* are associated with this disorder. We identified two types of *SCN5A* mutation in IVF patients (Fig. 4): some patients carry a missense mutation that leads to altered *SCN5A* function, and others seem to carry loss-of-function mutations. It is unclear how two types of mutation with different functional effects on sodium channels can lead to a similar IVF syndrome: both types cause ventricular fibrillation in individuals with a structurally normal heart, presumably as a result of re-entrant mechanisms; however, ECGs showing ST segment elevation and RBBB are not homogeneous—the ST segment elevation may exist only as J-point elevation<sup>30</sup> (as in family K005) or as complete ST segment elevation (as in family K007). Whether these differences in the ECG pattern are due to specific mutations or other modifying factors is unknown, and careful phenotype–genotype correlation of more IVF families is needed to clarify this further. Genetic testing and a mechanistic understanding of IVF may lead to rational therapies for cardiac arrhythmias. □

## Methods

**Identification and phenotyping of kindreds with IVF.** IVF kindreds were ascertained from medical clinics in North America, Germany, Spain, Italy and Belgium. Phenotypic criteria were identical to those used previously<sup>7,8</sup>. Diagnosis was defined by previous history of sudden death in probands or in a family member, no demonstrable structural heart disease or long-QT syndrome by invasive and non-invasive procedures, and an ECG pattern of RBBB and ST segment elevation in leads V1–V3 at baseline or after intravenous Ajmaline, as described previously<sup>7–10</sup>. The proband in K005 had a twin brother who died at the age of 23 years from IVF. In K007, the three brothers died of IVF at ages of 43, 46 and 35 years, respectively. The father of the proband had two syncopal episodes at ages 20 and 34 years before his fatal episode one year later.

The proband in K2823 had four syncopal episodes, which was diagnosed as IVT. The proband's father died suddenly from cardiac arrest at the age of 48 years, and a cousin died from a heart attack at the age of 27 years. IVT experienced by the proband was inducible by electrophysiological studies, and degenerated into ventricular fibrillation which required direct current cardioversion. The proband did not present the typical ECG pattern of RBBB and ST segment elevation at baseline.

**SSCP and DNA sequence analyses.** SSCP and DNA analyses were done as before<sup>23,24</sup> using PCR primers described previously<sup>18</sup>.

with each domain containing six transmembrane segments (S1–S6). IVF mutations are shown in green and LQT-associated mutations are in red.

**Electrophysiological characterization of human cardiac sodium channels.** Site-directed mutagenesis, *in vitro* transcription, *Xenopus* oocyte injection, electrophysiology, and data analysis were carried out as described<sup>26</sup>. Activation was estimated from current–voltage families evoked by step pulses of –50 to +50 mV (10-mV increment) from a holding potential at –100 mV. Peak test pulse currents were converted to conductances ( $G = I/(V - V_{rev})$ , where  $G$  is the conductance,  $I$  is the peak current,  $V$  is the test pulse and  $V_{rev}$  is the measured reversal potential). Conductance was normalized against the maximum observed in each cell and the mean values at each test potential were plotted. Inactivation was determined using a standard two-pulse protocol in which a 500-ms conditioning potential to varying levels (–120 to 0 mV) was followed by a test step to –10 mV (20 ms) to assess the extent of inactivation produced during the conditioning step. Test pulse currents were normalized to the maximum observed current (at the most negative conditioning potentials) and mean values  $\pm$ s.e.m. were plotted as a function of conditioning pulse amplitude. The time course of recovery from inactivation was measured using a three-pulse protocol in which a 500-ms conditioning pulse ( $V_c$ ) to –10 mV, allowing complete inactivation, was followed by a variable recovery interval ( $V_r$ ). Peak current evoked by test pulse ( $V_t$ ; –10 mV, 20 ms) was used to assay the amount of recovery. The envelope of superimposed test pulse currents was plotted versus the duration of the recovery interval and fitted to single exponential decay functions. The holding potential ( $V_h$ ) was –120 mV.

Received 29 September; accepted 23 December 1997.

1. Kannel, W. B., Cupples, A. & D'Agostino, R. B. Sudden death risk in overt coronary heart disease: the Framingham study. *Am. Heart J.* **113**, 799–804 (1987).
2. Willich, S. et al. Circadian variation in the incidence of sudden cardiac death in the Framingham heart study population. *Am. J. Cardiol.* **60**, 801–806 (1987).
3. Trappe, H. J. et al. Prognosis of patients with ventricular tachycardia and ventricular fibrillation: role of the underlying etiology. *J. Am. Coll. Cardiol.* **12**, 166–174 (1988).
4. Viskin, S. & Belhassen, B. Idiopathic ventricular fibrillation. *Am. Heart J.* **120**, 661–671 (1990).
5. Wichter, T., Breithardt, G. & Borggrefe, M. In *Cardiac Arrhythmia: Mechanism, Diagnosis, and Management* (eds Podrid, P. J. & Kowey, P. R.) 1219–1238 (Williams & Wilkins, Maryland, 1995).
6. Martini, B. et al. Ventricular fibrillation without apparent heart disease: description of six cases. *Am. Heart J.* **118**, 1203–1209 (1989).
7. Brugada, J., Brugada, R. & Brugada, P. Right bundle branch block, ST segment elevation in leads V1–V3: a marker for sudden death in patients without demonstrable structural heart disease. *Circulation* **96**, 1151 (1997).
8. Brugada, P. & Brugada, J. Right bundle branch block, persistent ST segment elevation and sudden cardiac death: a distinct clinical and electrocardiographic syndrome. A multicenter report. *J. Am. Coll. Cardiol.* **20**, 1391–1396 (1992).
9. Brugada, P. & Brugada, J. Further characterization of the syndrome of right bundle branch block, ST segment elevation, and sudden cardiac death. *J. Cardiovasc. Electrophysiol.* **8**, 325–331 (1997).
10. Brugada, J., Brugada, P. & Brugada, R. Ajmaline unmasks right bundle branch block-like and ST segment elevation in V1–V3 in patients with idiopathic ventricular fibrillation. *PACE* **19**, 599 (1996).
11. Miyanuma, H., Sakurai, M. & Odaka, H. Two cases of idiopathic ventricular fibrillation with interesting electrocardiographic findings. *Kokyu to Junkan* **41**, 287–291 (1993).
12. Aizawa, Y. et al. Idiopathic ventricular fibrillation and bradycardia-dependent intraventricular block. *Am. Heart J.* **126**, 1473–1474 (1993).
13. Sumiyoshi, M. et al. A case of idiopathic ventricular fibrillation with incomplete right bundle branch block and persistent ST segment elevation. *Jpn Heart J.* **34**, 661–666 (1993).

14. Bjerregaard, P., Gussak, I., Kotar, S. L., Gessler, J. E. & Janosik, D. Recurrent syncope in a patient with prominent J wave. *Am. Heart J.* **127**, 1426–1430 (1994).
15. Miyazaki, T. *et al.* Autonomic and antiarrhythmic drug modulation of ST segment elevation in patients with Brugada syndrome. *J. Am. Coll. Cardiol.* **27**, 1061–1070 (1996).
16. Tung, R. T., Shen, W., Hammil, S. C. & Gersh, E. J. Idiopathic ventricular fibrillation in out-of-hospital cardiac arrest survivors. *PACE* **17**, 1405–1411 (1994).
17. Cobb, L. A. in *Hurst's The Heart* (eds Schlant, R. C. & Alexander, R. W.) 8th edn. 947–957 (McGraw Hill, New York, 1994).
18. Wang, Q., Li, Z., Shen, J. & Keating, M. T. Genomic organization of the human *SCN5A* gene encoding the cardiac sodium channel. *Genomics* **34**, 9–16 (1996).
19. Rogers, J. C., Qu, Y., Tanada, T. N., Scheuer, T. & Catterall, W. A. Molecular determinants of high affinity binding of  $\alpha$ -scorpion toxin and sea anemone toxin in the S3–S4 extracellular loop in domain IV of the Na channel  $\alpha$  subunit. *J. Biol. Chem.* **271**, 15950–15962 (1996).
20. Hoffman, E. P., Lehmann-Horn, F. & Rudel, R. Overexcited or inactive: ion channels in muscle disease. *Cell* **80**, 681–686 (1995).
21. Yang, N. & Horn, R. Evidence for voltage-dependent S4 movement in sodium channels. *Neuron* **15**, 213–218 (1995).
22. Shapiro, M. B. & Senapathy, P. RNA splice junctions of different classes of eukaryotes: sequence statistics and functional implications in gene expression. *Nucleic Acids Res.* **15**, 7155–7174 (1987).
23. Wang, Q. *et al.* *SCN5A* mutations associated with an inherited cardiac arrhythmia, long QT syndrome. *Cell* **80**, 805–811 (1995).
24. Wang, Q. *et al.* Cardiac sodium channel mutations in patients with long QT syndrome, an inherited cardiac arrhythmia. *Hum. Mol. Genetics* **4**, 1603–1607 (1995).
25. Bennett, P. B., Yazawa, K., Makita, N. & George, A. L. Jr Molecular mechanism for an inherited cardiac arrhythmia. *Nature* **376**, 683–685 (1995).
26. Dumaine, R. *et al.* Multiple mechanisms of Na<sup>+</sup> channel-linked long-QT syndrome. *Circulation Res.* **78**, 916–922 (1996).
27. Stuhmer, W. *et al.* Structural parts involved in activation and inactivation of the sodium channel. *Nature* **339**, 597–603 (1989).
28. Krishnan, S. C. & Antzelevitch, C. Sodium channel block produces opposite electrophysiological effects in canine ventricular epicardium and endocardium. *Circulation Res.* **69**, 277–291 (1991).
29. Krishnan, S. C. & Antzelevitch, C. Flecainide-induced arrhythmia in canine ventricular epicardium. Phase 2 reentry? *Circulation* **87**, 562–572 (1992).
30. Yan, G. X. & Antzelevitch, C. Cellular basis for the electrocardiographic J wave. *Circulation* **93**, 372–379 (1996).

**Acknowledgements.** We thank H. Hartmann for the wild-type *SCN5A* construct; M. Sanguinetti and P. Spector for help with electrophysiological analysis of the 1-bp deletion; and P. Szafranski, J. T. Bricker, M. Scheinman, A. L. Beaudet, A. Bradley and X. Qu for help and advice. This work was supported by a Grant-In-Aid from the American Heart Association, by the AHA, Northeast Ohio Affiliate (G.E.K.), and the Deutsche Forschungsgemeinschaft (E.S.-B.), and by grants from the NIH and Bristol-Myers Squibb (M.T.K.), The Texas Children's Hospital Foundation Chair in Pediatric Cardiac Research and NIH grants (J.A.T.), the Carolien Weiss Law Grant for Research in Molecular Medicine (Q.W.), the Abercrombie Cardiology Fund of Texas Children's Hospital (Q.W.), and a Scientist Development Award from the American Heart Association (Q.W.).

Correspondence and requests for materials should be addressed to Q.W. (e-mail: qwang@bcm.tmc.edu).

## Fas-mediated apoptosis and activation-induced T-cell proliferation are defective in mice lacking FADD/Mort1

Jianke Zhang, Dragana Cado, Ann Chen, Nisha H. Kabra & Astar Winoto

Department of Molecular and Cell Biology, Division of Immunology and Cancer Research Laboratory, University of California at Berkeley, 469 LSA, Berkeley, California 94720-3200, USA

Programmed cell death, or apoptosis, is important in homeostasis of the immune system: for example, non-functional or auto-reactive lymphocytes are eliminated through apoptosis. One member of the tumour necrosis factor receptor (TNFR) family, Fas (also known as CD95 or Apo-1), can trigger cell death and is essential for lymphocyte homeostasis<sup>1,2</sup>. FADD/Mort1 (refs 3–6) is a Fas-associated protein that is thought to mediate apoptosis by recruiting the protease caspase-8 (refs 7, 8). A dominant-negative mutant of FADD inhibits apoptosis initiated by Fas and other TNFR family members<sup>6,9–14</sup>. Other proteins, notably Daxx, also bind Fas and presumably mediate a FADD-independent apoptotic pathway<sup>15</sup>. Here we investigate the role of FADD *in vivo* by generating FADD-deficient mice. As homozygous mice die *in utero*, we generated *FADD*<sup>-/-</sup> embryonic stem cells and *FADD*<sup>-/-</sup> chimaeras in a background devoid of the recombination activating gene *RAG-1*, which activates rearrangement of the immunoglobulin and T-cell receptor genes. We found that thymocyte subpopulations were apparently normal in newborn chimaeras.

Fas-induced apoptosis was completely blocked, indicating that there are no redundant Fas apoptotic pathways. As these mice age, their thymocytes decrease to an undetectable level, although peripheral T cells are present in all older *FADD*<sup>-/-</sup> chimaeras. Unexpectedly, activation-induced proliferation is impaired in these *FADD*<sup>-/-</sup> T cells, despite production of the cytokine interleukin (IL)-2. These results and the similarities between *FADD*<sup>-/-</sup> mice and mice lacking the  $\beta$ -subunit of the IL-2 receptor suggest that there is an unexpected connection between cell proliferation and apoptosis.

To generate FADD-deficient mice we replaced the first exon of FADD with a neomycin-resistance (neo) gene (Fig. 1a). Heterozygous mutant embryonic stem (ES) cells were identified by Southern blot analysis (Fig. 1b), and *FADD*<sup>+/-</sup> mice were produced from three *FADD*<sup>+/-</sup> ES lines. Interbreeding of these mice, however, yielded only heterozygous and wild-type mice in a 2:1 ratio. Subsequent studies established that *FADD*<sup>-/-</sup> embryos die at around day 9 of gestation (data not shown), indicating that FADD is essential for embryonic development.

Because Fas is necessary for homeostasis in the immune system, we sought to investigate the effect of FADD deletion in lymphoid organs. However, this can not be examined directly because *FADD*<sup>-/-</sup> mice die *in utero*. We therefore made *FADD*<sup>-/-</sup> ES cells and injected them into C57BL/6-*RAG-1*<sup>-/-</sup> (B6-*RAG-1*<sup>-/-</sup>) blastocysts to generate *FADD*<sup>-/-</sup> chimaeras<sup>16</sup>. Homozygous *FADD*<sup>-/-</sup> ES cells were obtained by subjecting *FADD*<sup>+/-</sup> ES cells to a high level of G418 selection<sup>17</sup> (Fig. 1b). Complete absence of FADD protein was confirmed by western blot analysis (Fig. 1c). Because these ES donor cells originate from 129/Sv strain (agouti colour) and host blastocysts originate from B6-*RAG-1*<sup>-/-</sup> mice (black), chimaeras were readily identified by coat colour. By this means we generated 20 viable chimaeras. All mature lymphocytes in these *FADD*<sup>-/-</sup> → *RAG-1*<sup>-/-</sup> chimaeras (designated *FADD*<sup>-/-</sup>) are derived from *FADD*<sup>-/-</sup> ES cells because *RAG-1*<sup>-/-</sup> mice are not capable of producing any B or T cells<sup>18</sup>. An antibody for the allelic Ly9.1 antigen provides another means of distinguishing the donor (129/Sv mice are Ly9.1<sup>+</sup>) from the host cells (B6 mice are Ly9.1<sup>-</sup>). Tissue Southern blot analysis confirmed the contribution of *FADD*<sup>-/-</sup> ES cells in many organs and tissues (data not shown).

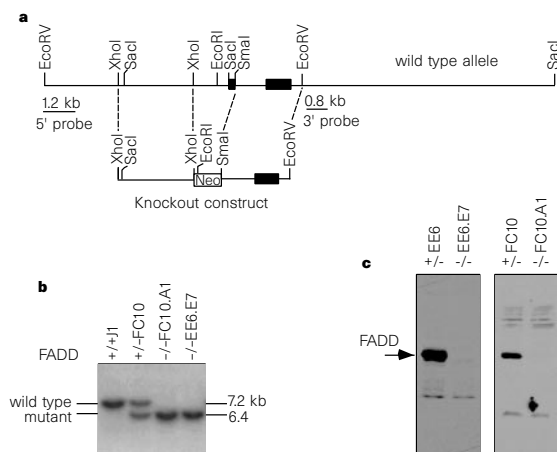


**Figure 1** Targeted inactivation of the gene encoding FADD/Mort1 in ES cells and in mice. **a**, A restriction map of the murine *FADD* locus is shown (filled boxes denote exons)<sup>6</sup>. A schematic representation of the FADD targeting construct is shown underneath. **b**, Generation of FADD-deficient ES cell clones. Heterozygous ES cell clones were identified by Southern blots with 5' probe which detects a 7.2-kilobase (*EcoRI*-*EcoRV*) wild-type allele and a 6.4-kb mutant allele. Two *FADD*<sup>-/-</sup> clones, FC10.A1 and EE6.E7, were obtained after further G418 selection<sup>17</sup>. They contain only the mutant alleles. J1 is the parental wild-type ES cell for FC10. **c**, The absence of FADD protein in *FADD*<sup>-/-</sup> lines was confirmed by western blot analysis using anti-FADD antibodies<sup>6</sup>.